

# Testing Newtonian Gravity with AAOmega: Mass-to-Light Profiles of Four Globular Clusters

Richard R. Lane<sup>1\*</sup>, László L. Kiss<sup>1</sup>, Geraint F. Lewis<sup>1</sup>, Rodrigo A. Ibata<sup>2</sup>,  
Arnaud Siebert<sup>2</sup>, Timothy R. Bedding<sup>1</sup> and Péter Székely<sup>3</sup>

<sup>1</sup>*Sydney Institute for Astronomy, School of Physics, A28, The University of Sydney, NSW, Australia 2006*

<sup>2</sup>*Observatoire Astronomique, Université de Strasbourg, CNRS, 67000 Strasbourg, France*

<sup>3</sup>*Department of Experimental Physics, University of Szeged, Szeged 6720, Hungary*

This draft: 29 October 2021

## ABSTRACT

Testing Newtonian gravity in the weak-acceleration regime is vital to our understanding of the nature of the gravitational interaction. It has recently been claimed that the velocity dispersion profiles of several globular clusters flatten out at large radii, reminiscent of galaxy rotation curves, even though globular clusters are thought to contain little or no dark matter. We investigate this claim, using AAOmega observations of four globular clusters, namely M22, M30, M53 and M68. M30, one such cluster that has had this claim made for its velocity dispersion, was included for comparison with previous studies. We find no statistically significant flattening of the velocity dispersion at large radii for any of our target clusters and therefore we infer the observed dynamics do not require that globular clusters are dark matter dominated, or a modification of gravity. Furthermore, by applying a simple dynamical model we determine the radial mass-to-light profiles for each cluster. The isothermal rotations of each cluster are also measured, with M22 exhibiting clear rotation, M68 possible rotation and M30 and M53 lacking any rotation, within the uncertainties.

**Key words:** gravitation - Galaxy: globular clusters: individual - stellar dynamics

## 1 INTRODUCTION

Newtonian gravitation has been shown to describe the motions of bodies with intermediate accelerations (e.g. Solar System bodies) very accurately. The Newtonian theory of gravity breaks down in the presence of strong gravitational fields, where it has been successfully superseded by General Relativity, but there is evidence that there are also discrepancies in the low-acceleration regime. Spiral galaxies, for example, require the invocation of Dark Matter (DM) to reconcile the discrepancy between their rotational velocities and our understanding of Newtonian gravity. Another indication is the so-called ‘‘Pioneer anomaly’’: radiometric data from Pioneers 10 and 11 have shown that both are experiencing an unexplained constant acceleration of  $a = (8.74 \pm 1.33) \times 10^{-10} \text{ m s}^{-2}$  toward the Sun (see de Diego 2008, and references therein). In fact, all spacecraft in the outer Solar System seem to be experiencing this anomalous acceleration (e.g. Anderson *et al.* 2002), potentially indicating a deviation from Newtonian gravity at low accelerations.

It has been claimed that one of the leading versions of

modified Newtonian dynamics (MOND; Milgrom 1983) can predict the kinematic properties of galaxies without invoking DM. MOND predicts a breakdown of Newtonian gravity at an acceleration scale  $a_0 \approx 1.2 \times 10^{-10} \text{ m s}^{-2}$  (see Iorio 2009, and references therein). This is approximately the acceleration regime where DM becomes necessary to reconcile theoretical velocity profiles of galaxies with observation.

Globular clusters (GCs) are the ideal test bed for this divergence from Newtonian predictions, since they are thought to contain little or no DM. This is based on evidence from dynamical models (e.g. Phinney 1993),  $N$ -body simulations (e.g. Moore 1996), observations of GC tidal tails (e.g. Odenkirchen *et al.* 2001), dynamical and luminous masses of GCs (e.g. Mandushev *et al.* 1991) and the lack of microlensing events from GC-mass dark haloes (e.g. Navarro *et al.* 1997; Ibata *et al.* 2002). In addition, GCs at different distances from the Galactic centre experience differing gravitational attractions from the Galaxy, so that any Galactic influence can be ruled out if all exhibit similar behaviour. Furthermore, the accelerations experienced by stars in GCs drop below  $a_0$  well inside the tidal radius (e.g. Scarpa *et al.* 2007).

Recently, Scarpa *et al.* (2007) showed that there may

\* E-mail: rlane@physics.usyd.edu.au

be a flattening of the velocity profiles of several GCs in the Galactic halo ( $\omega$  Centauri, M15, M30, M92 and M107), at or about the acceleration where DM is invoked to maintain stability in rotating galaxies. On the other hand, Moffat & Toth (2008) overlaid the Scarpa *et al.* (2007) results with a Modified Gravity (MOG) model and found little, or no, deviation from Newtonian gravity, for GCs with masses less than a few times  $10^6 M_{\odot}$ . Because both groups used an identical set of measured velocity dispersions, there is an obvious discrepancy. If MOND were correct, it would mean that all gravitational interactions would diverge from Newtonian gravitation in the predicted regime. Irrespective of MOND itself, testing the gravitational interaction at low accelerations is extremely important in the overall understanding of gravity. This paper continues this test, with four Galactic halo GCs, namely M22 (NGC 6656), M30 (NGC 7099), M53 (NGC 5024) and M68 (NGC 4590).

## 2 DATA ACQUISITION AND REDUCTION

We used the multi-object, double-beam spectrograph (AAOmega) on the 3.9 m Anglo-Australian Telescope at Siding Spring Observatory in New South Wales, Australia, to obtain the spectra for this survey. AAOmega has 392 fibres covering a 2 square degree field of view with each fibre capable of obtaining a single spectrum from a single star in this field. The 1500V grating (with a resolution of  $R = 3700$ ) was used in the blue arm and the 1700D grating ( $R = 10000$ ) was used in the red arm, with the central wavelengths set to 5200Å and 8640Å, respectively. This configuration was chosen to include the calcium triplet lines at 8498Å, 8542Å and 8662Å, for accurate velocity determination and proxy metallicities, as well as the swathe of iron and magnesium lines around 5200Å for accurate metallicity measurements. The astrometric positions of the targets, taken from the 2MASS Point Source Catalogue<sup>1</sup>, have accuracies of  $\sim 0.1''$ .

The observations were taken over two observing runs, on 5–8 and 14–19 June 2008, with an average seeing of  $\sim 1.5''$ . We obtained  $3 \times 1200$ -second exposures per fibre configuration, to obtain  $S/N \sim 20 - 100$ , with several configurations per cluster (see Table 1 for actual numbers of spectra obtained for each cluster – note that for M68, 3 configurations were obtained in June 2008, and 5 further configurations were obtained during a separate service run in May 2009). In this study we also made use of data for M30 obtained in a previous observing run in 2006 (originally published by Kiss *et al.* 2007). Flat fields, arc lamp exposures and  $\sim 25$  dedicated sky fibres were used for data reduction and calibration. FeAr, CuAr, CuHe, CuNe and ThAr arc lamps were used to ensure accurate wavelength calibration. Data reduction was performed using the **2dfdr** pipeline<sup>2</sup>, designed specifically for the reduction of AAOmega data. The efficacy of the pipeline has been checked with a comparison of individual stellar spectra.

**Table 1.** Clusters selected for the current survey, based on the criteria outlined in the text, with the total number of fibre configurations, and spectra, obtained during the run. Note that the number of spectra quoted here is the total number of spectra obtained before Galactic contaminants were removed. For M68, 3 configurations were observed on the two observing runs in June 2008 and 5 subsequent configurations were observed during a service run in May 2009.

Cluster	# Fibre Configurations	Total # Spectra
M22	10	3407
M30	2	620
M53	6	1727
M68	3+5	2650

### 2.1 Cluster Selection

We aimed to observe several hundred stars from each of four GCs, namely M22 (NGC 6656), M30 (NGC 7099), M53 (NGC 5024) and M68 (NGC 4590). These four targets were selected by several criteria: they are bright ( $M_V < -7$ ), nearby ( $D < 30$  kpc) and have radial velocities  $> 1.5\sigma$  from the peak velocity given by the Besançon Galaxy Model<sup>3</sup> in that direction, for ease of extracting the cluster members from Galactic contaminants. One cluster (M30) was included specifically because it was one of the targets of Scarpa *et al.* (2007), and it satisfied all other selection criteria. This allows a comparison with the results of that study.

We produced a Colour Magnitude Diagram (CMD) for each cluster using data from the 2MASS Point Source Catalogue, and the Red Giant Branch (RGB) was identified in colour-magnitude space. Selection of individual target stars was based on the  $J - K$  colours and  $K$  magnitudes of the RGB of the cluster to minimise the number of stars selected from the Galactic population. Despite this selection process, a number of Galactic contaminant stars were still expected in the final sample and it was therefore necessary to remove them before analysis. Section 2.1.1 describes this process.

#### 2.1.1 Cluster Membership

To select cluster members, it was necessary to determine several quantities for each observed star. Atmospheric parameters and radial velocities were determined using an iterative process, combining best fits to the synthetic spectra from the Munari *et al.* (2005) spectrum library, with  $\chi^2$  fitting, and cross-correlating this best fit model with the observed spectrum to calculate the radial velocity. This approach is very similar to that adopted by the Radial Velocity Experiment (RAVE) project (Steinmetz *et al.* 2006; Zwitter *et al.* 2008), and is based on the same synthetic spectral library as RAVE. Kiss *et al.* (2007) outlined this method in detail.

For M22, M30 and M68, we used four parameters to identify members, namely metallicity ( $[m/H]$ ), equivalent width of the calcium triplet lines, radial velocity and the distance from the centre of the cluster [terminating at the tidal radius as quoted by Harris (1996)]; only stars that matched using all criteria were judged to be members. Figure 1 shows

<sup>1</sup> <http://www.ipac.caltech.edu/2mass/>

<sup>2</sup> <http://www.aao.gov.au/2df/software.html#2dfdr>

<sup>3</sup> <http://www.obs-besancon.fr/modele/>

all the stars for which spectra were obtained, highlighting those determined to be cluster members. Note that spectra from observing runs over 2006–2008 were combined with the spectra of M22, M30 and M68 taken during the current survey to ensure greater statistical significance of the results.

M53, being closer to the Galaxy in both  $[m/H]$  and radial velocity, required a non-degenerate metallicity to determine membership. We used the method outlined by Cole *et al.* (2004) to calculate  $[Fe/H]$  from the equivalent widths of the calcium triplet lines for each star, resulting in a much cleaner selection for this cluster. Further cuts were made on temperature ( $T_{\text{eff}} < 9000$  K) and the quality of the synthetic spectral fit to produce the final sample used for analysis. Typical uncertainties in the radial velocities of our member stars are  $\sim 3 \text{ km s}^{-1}$ ,  $\sim 2 \text{ km s}^{-1}$ ,  $\sim 3 \text{ km s}^{-1}$  and  $\sim 2.5 \text{ km s}^{-1}$ , for M22, M30, M53 and M68, respectively. All stars have uncertainties less than  $6 \text{ km s}^{-1}$ .

The sample consisted of 345, 194, 180 and 123 RGB member stars for M22, M30, M53 and M68 respectively. Note that for M30, the 168 Main Sequence Turn Off (MSTO) and sub-giant branch stars from the Scarpa *et al.* (2007) study were also included in our analysis, bringing the total number of members for that cluster to 362. The consequence of mixing stellar types in our analysis of M30 is discussed in Section 3.2.

### 3 RESULTS

#### 3.1 Rotation

The radial velocities were used to determine the rotation of each cluster, assuming an isothermal rotation. The rotation was measured by dividing the cluster in half at a given position angle (PA) and calculating difference between the average velocities in the two halves. This was performed over PAs in steps of  $10^\circ$  for all clusters, except M53 was done in  $15^\circ$  steps to avoid aliasing effects. The resulting data were then fit with a sine function. Figure 2 shows the measured rotation for each cluster and the best-fit sine function. Note that Scarpa *et al.* (2007) detected no rotation in M30 to a level of  $0.75 \text{ km s}^{-1}$  and we corroborate their result; we detect no evidence for rotation to a level of  $0.8 \text{ km s}^{-1}$ . For M53, no rotation is evident to  $0.5 \text{ km s}^{-1}$ , however, it is clear that M22 is rotating, with a projected axis of rotation approximately North-South. M68 shows some indication of rotation, although additional data are required to confirm this.

#### 3.2 Velocity Dispersions

To determine the velocity dispersions of our samples, we first corrected all four clusters for rotation, and then binned the stars by distance from the cluster centre (annuli), ensuring approximately equal numbers of stars per bin. The mean and standard deviation were calculated for the velocities in each bin. Our velocity dispersions were determined using a Markov Chain Monte Carlo maximum likelihood method (see Gregory 2005 for an overview of MCMC methodology), which takes into account the individual velocity uncertainties on the stars and provides the velocity dispersion in each bin with associated uncertainties.

The resulting velocity dispersion profiles were then over-plotted with the best-fitting Plummer (1911) model, as shown in Figure 3. The data points have been plotted at the mean radius of the stars in each bin. Because fewer cluster members exist at larger radii, the outermost bin is generally much larger than the inner bins. To ensure our Plummer model fits do not exhibit an artificial slope in the outskirts of the clusters, masking any possible flattening of the velocity dispersion profiles, we also performed fits to the profiles with the last bin excluded. The fits are nearly identical for M22, M30 and M68. For M53 a small discrepancy between the fits was observed due to the scatter in the velocity dispersions of the inner bins, however, this discrepancy has no impact on our overall results. The reduced  $\chi^2$  values for the Plummer fits shown in Figure 3 are  $\sim 2.3$ ,  $\sim 1.1$ ,  $\sim 2.0$  and  $\sim 1.5$  for M22, M30, M53 and M68, respectively. We used two parameters in the fitting process, namely the central velocity dispersion and the scale radius ( $r_s$ ; containing half the cluster mass). Due to the nature of the model it is possible to calculate the total cluster mass from the central velocity dispersion ( $\sigma_0$ ) and  $r_s$  (see Dejonghe 1987 for a detailed discussion of Plummer models and their application):

$$M_{\text{tot}} = \frac{64\sigma_0^2 r_s}{3\pi G}.$$

The total masses are shown in each panel of Figure 3.

We chose the Plummer model to fit to our velocity dispersion profiles because it is a monotonically decreasing function and, therefore, any flattening of the profiles would be clearly shown. The cluster in common between this study and that of Scarpa *et al.* (2007), M30, shows the best Plummer fit of the four. Note that our complete dataset, which includes those data used by Scarpa *et al.* (2007), has been binned to ensure similar numbers of stars per bin. Because our binning is different to that used by Scarpa *et al.* (2007), a data point-by-data point comparison between the two studies is not possible here. Within the limits of the model, and the uncertainties in the data, the velocity dispersion does not exhibit any flattening at large radii, and therefore there is no indication that either DM or a modified theory of gravity is required to explain the velocity dispersion of M30. The same case can be made for the other three clusters we examined, and the velocity dispersion profiles, along with best fit Plummer models (and parameters) are presented in Figure 3.

Different stellar populations in GCs are known to have differing velocity scatters within the cluster (“velocity jitter”; see Gunn & Griffin 1979; Carney *et al.* 2003, for detailed discussions). This jitter is due to instabilities in the atmospheres of luminous giant stars. Since we included the MSTO and sub-giant stars from the Scarpa *et al.* (2007) study with our RGB sample, this jitter should be evidenced as a slightly increased velocity dispersion from the result by Scarpa *et al.* (2007). This increase in dispersion will be smaller, however, than if we produced our velocity dispersions from our RGB stars alone. Comparing our dispersion profiles for M30 with those of Scarpa *et al.* (2007), we see some evidence for this increase in the inner regions of the cluster, although the difference is well within the uncertainties. No increase in dispersion is seen in the outer parts; Scarpa *et al.* (2007) quote a dispersion of  $\sim 2.25 \text{ km s}^{-1}$  at a radius of 25 pc, whereas our data show a dispersion of

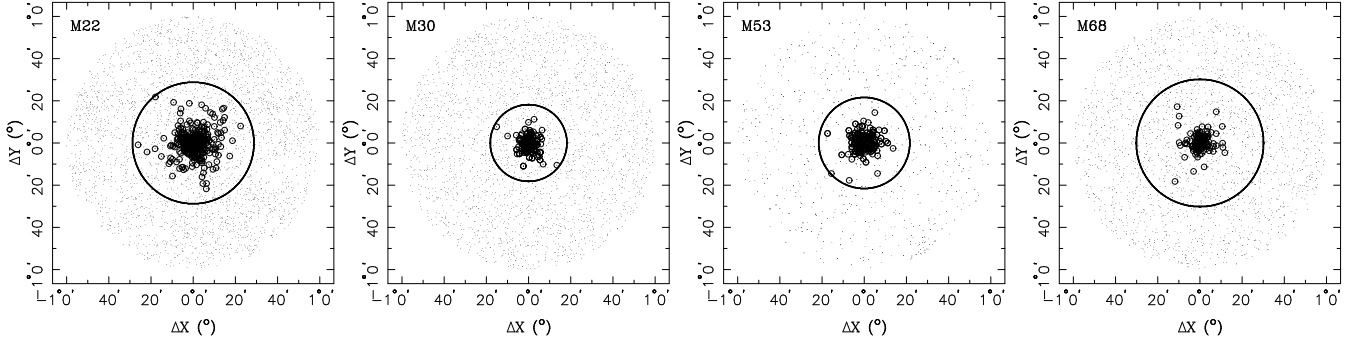


**Figure 1.** Members of each cluster used for analysis (circled dots), based on the selection method described in the text. The uncircled dots are the stars which were observed and determined not to be cluster members. The large circle is the tidal radius of the cluster from Harris (1996). In each panel, North is up and East is to the left.

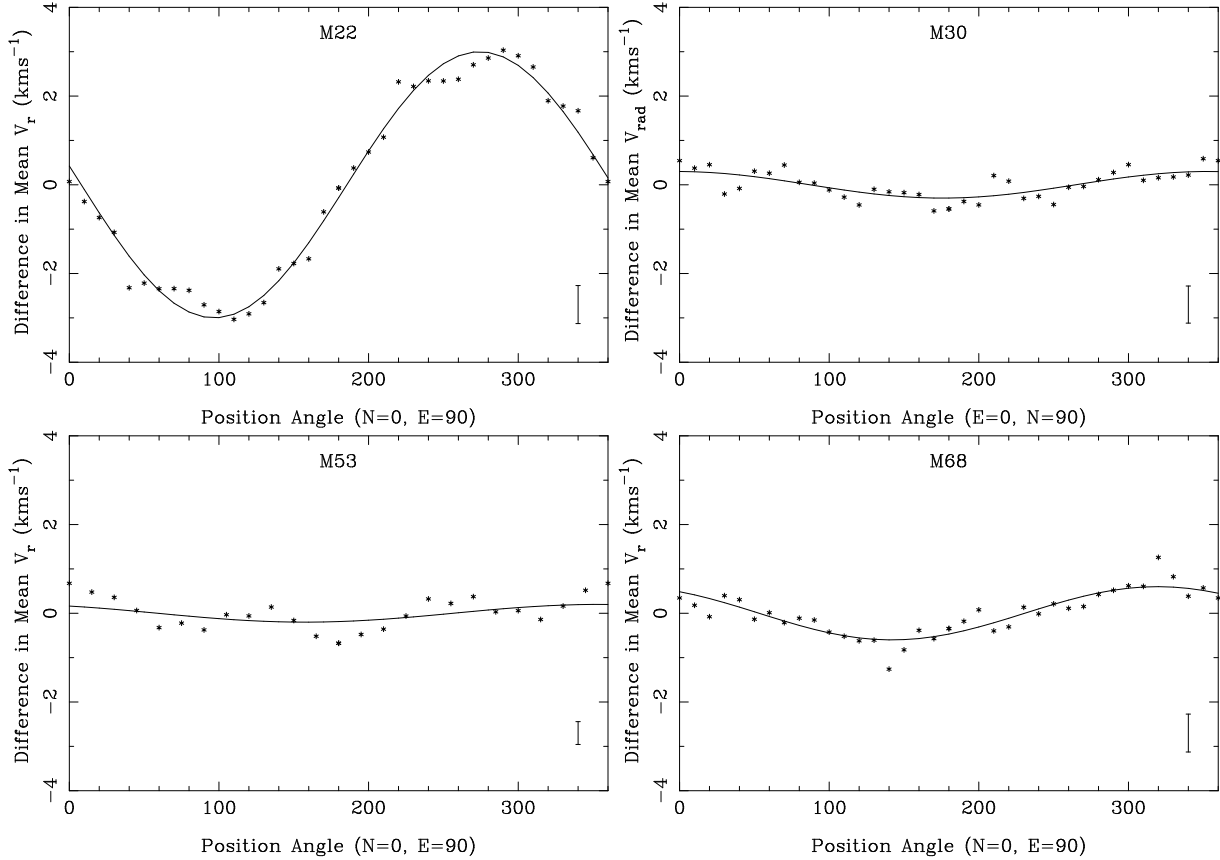


**Figure 2.** The rotation of each cluster calculated as the difference between the mean velocities from each side of the cluster along equal position angles, as described in the text. The best  $\chi^2$  fit sine function is overplotted, and a typical error bar is represented in the lower right of each panel.

$\sim 1.6 \text{ km s}^{-1}$  at this distance, although this discrepancy is still within the uncertainties.

The main result from the Scarpa *et al.* (2007) study was an apparent flattening of the velocity dispersion profiles of five of their six clusters, indicating a DM component, or a need for a modified gravity theory to explain their results. Moffat & Toth (2008) overlaid the dispersion profiles of Scarpa *et al.* (2007) with a MOG dispersion profile and showed that the flattening of the profiles was consistent with Newtonian gravity, although the authors did omit one data point from two of the clusters analysed. The Moffat & Toth

(2008) MOG model differs from Newtonian gravity for very massive objects (e.g. galaxy clusters and elliptical galaxies) but becomes Newtonian for masses below a few times  $10^6 M_{\odot}$ , which is the mass range of GCs. The MOG fit proves to be an equivalently good fit to these data, indicating no deviation from Newtonian gravity in these clusters, and a Gaussian with a flat tail has no physical significance. Because Scarpa *et al.* (2007) overlaid their data with a Gaussian with a flat tail, and Moffat & Toth (2008) overlaid the same data with a MOG model (which becomes Newtonian at low mass), and both are a similarly good fit, neither DM

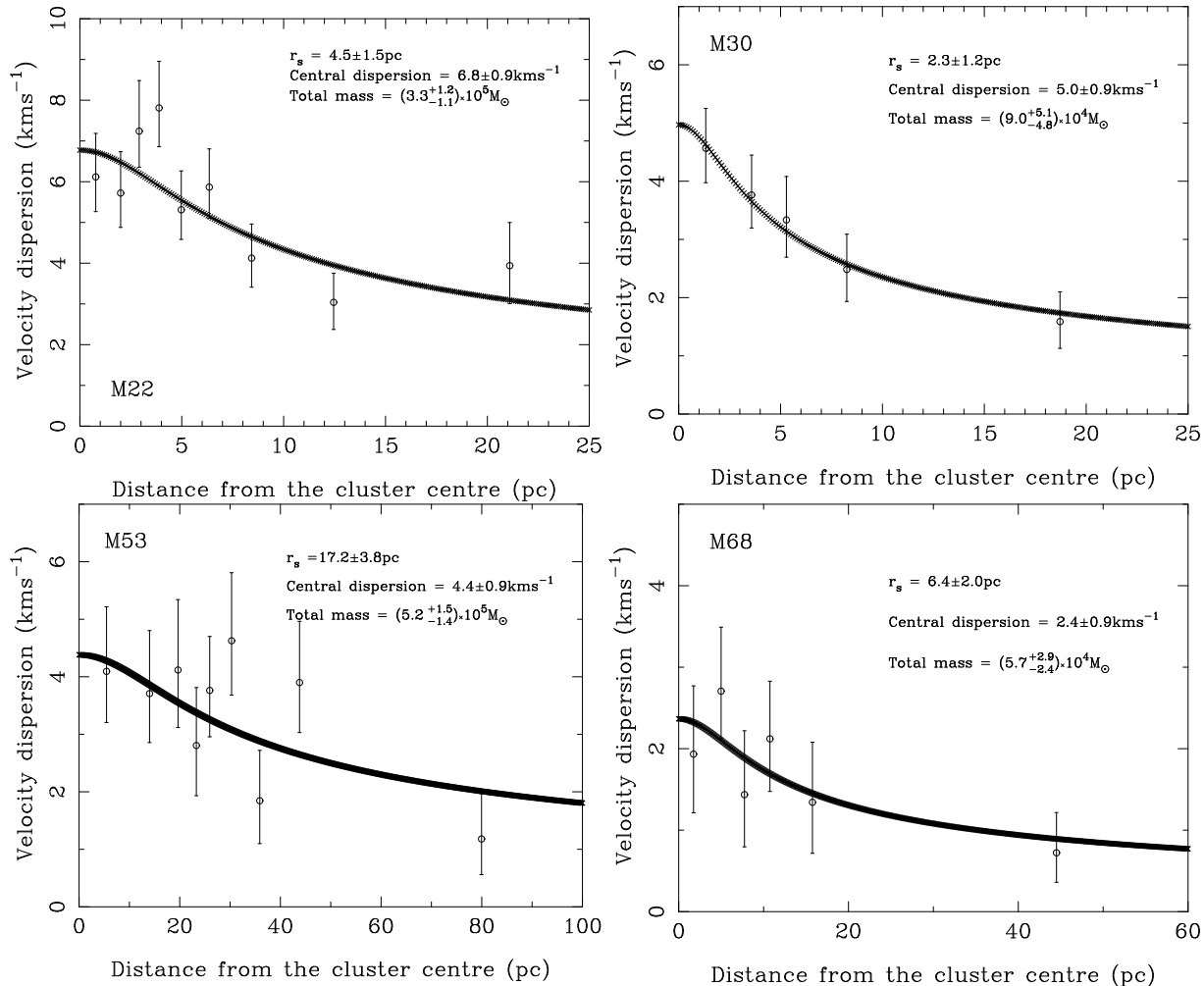


**Figure 3.** Velocity dispersion profiles of each cluster. The best fitting Plummer (1911) model is overplotted, and the fitted parameters as well as the calculated total cluster mass is shown.

nor a modified version of gravity are required to explain their data, and our study confirms this.

### 3.3 Systemic Velocities

In addition to the velocity dispersions, the systemic velocity of each cluster was measured (using the Monte Carlo method described above) and compared to similar data in Harris (1996), the most comprehensive catalogue of GC parameters. This comparison is summarised in Table 2. Note especially M53, for which our calculated velocity is significantly different to that of Harris (1996), with the discrepancy well outside the error bars of both measurements. Since Harris (1996) quotes systemic velocity data for M53 from Webbink (1981), who examined a total of 12 stars, our systemic velocity calculation based on 180 stars is a more reliable measurement for this cluster.

### 3.4 Mass-to-Light Ratio

One important indicator of large quantities of DM in a dynamical system is a large mass-to-light ratio (i.e.  $M/L_V \gg 1$ ).

**Table 2.** Comparisons between the radial velocities of each cluster in the Harris (1996) catalogue and those from this survey.

Cluster	$V_r$ (Harris 1996)	$V_r$ (this paper)
M22	$-148.9 \pm 0.4$	$-144.86 \pm 0.34$
M30	$-181.9 \pm 0.5$	$-184.40 \pm 0.20$
M53	$-79.1 \pm 4.1$	$-62.80 \pm 0.31$
M68	$-94.3 \pm 0.4$	$-94.93 \pm 0.26$

Furthermore, this DM will cause the stars to have large accelerations, and therefore inherently higher maximal velocities, and hence a larger velocity dispersion. An obvious way to determine whether or not a pressure-supported object like a GC is dark matter dominated is to measure its  $M/L_V$ . Of course, this requires a surface brightness profile, for which we have used those by Trager *et al.* (1995). These profiles were converted to solar luminosities per square parsec. The density profile was then calculated using (again, see Dejonghe 1987):

$$\rho(r) = \frac{M_{tot}}{\pi} \frac{r_s^2}{(r_s^2 + r^2)^2}.$$

The  $M/L_V$  profiles are shown in Figure 4, along with the  $M/L_V$  ratios. The vertical line shows the value of  $r_s$ . Because the central regions of GCs are highly concentrated, particularly in post-core-collapsed clusters, it is difficult to accurately determine the mass in the core. The  $M/L_V$  ratios have, therefore, only been calculated for radii greater than  $r_s$ . Evstigneeva *et al.* (2007) showed that ultra-compact dwarf galaxies (UCDs) follow the same luminosity – velocity dispersion relation as old GCs. Since it has also been shown that UCDs with a dynamical  $M/L_V$  up to 5 do not require dark matter to explain these mass-to-light ratios (e.g. Hasegan *et al.* 2005; Evstigneeva *et al.* 2007), we see no requirement for any of our clusters, apart from M53, to contain any dark matter component. Hasegan *et al.* (2005) determined that a  $M/L_V > 6$  for UCDs may indicate some dark matter content, and since we estimate  $M/L_V \approx 6.7$  for M53, this may indicate a small dark matter component in this cluster. Note that if we take the lower limit of our uncertainties for the mass-to-light ratio of M53 we reach the regime where dark matter is not required, and none of our clusters show  $M/L_V \gg 1$ , indicating DM is not dominant.

Note that we have produced  $M/L_V$  profiles rather than simply deriving a single  $M/L_V$  value from the central velocity dispersion and central surface brightness. We suggest that determining  $M/L_V$  profiles is preferable because it describes the  $M/L_V$  of the entire cluster outside the core, rather than just its core. This is especially true for post-core-collapse clusters, such as M30, in which the core masses are highly uncertain. Furthermore, M30 is the only cluster in our sample known to have a collapsed core (e.g. Trager *et al.* 1995). This cluster also has a maximum in its  $M/L_V$  profile at about the scale radius  $r_s$ , which may be due to mass segregation. The most massive stars are known to fall toward the core during the evolution of the cluster (see Spitzer 1985, for a review of mass segregation processes in GCs). The somewhat less pronounced maximum in the  $M/L_V$  profile of M68 may be the first evidence that this cluster is currently undergoing core collapse. It has been argued that a central concentration parameter  $c \approx 2$  may indicate a collapsed core in certain GCs, and for M68  $c = 1.91$  (van den Bergh 1995). Note that, despite our calculation of the  $M/L_V$  ratio being restricted to  $R > r_s$ , the profiles should be accurate for  $R > r_c$ , the core radius, or  $R \gtrsim r_s/2$ . Therefore, we argue that the peak in  $M/L_V$  is real, although a larger sample of cluster members for  $R < r_s$  will be required to test this and, therefore, to show whether M68 is truly undergoing core collapse.

#### 4 CONCLUSIONS

We have studied four GCs to determine their velocity dispersion profiles, and found that neither DM nor modified gravity are required to reconcile the kinematic properties of these particular clusters. M53 may contain a small DM component, indicated by a  $M/L_V > 6$ , but it is not dominant. Within the uncertainties, the  $M/L_V$  ratio of M53 is still consistent with little, or no, DM content. The dynamics of all four clusters are well described by a purely analytic Plummer (1911) model, which indicates that Newtonian gravity adequately describes their velocity dispersions, and shows no breakdown of Newtonian gravity at

$a_0 \approx 1.2 \times 10^{-10} \text{ m s}^{-2}$ , as has been claimed in previous studies.

Furthermore, the Plummer model was used to determine the total mass, scale radius (the radius at which half the mass is contained), and the  $M/L_V$  profile for each cluster. We find that none of our clusters have  $M/L_V \gg 1$ , another indication that DM is not dominant. Within the uncertainties, our estimated cluster masses all match those in the literature (e.g. Meziane & Colin 1996), and the same is true for the  $M/L_V$  ratios (e.g. Pryor & Meylan 1993). We have produced  $M/L_V$  profiles, rather than quoting a single value based on the central velocity dispersion and central surface brightness. This method is preferred because it describes the  $M/L_V$  of the entire cluster, rather than only its core; this is particularly important for post-core-collapsed GCs for which the central mass is highly uncertain.

Because the only known of our clusters to have a collapsed core (M30) shows a peak in its  $M/L_V$  profile at approximately  $r_s$ , this may be an indication of the resulting mass segregation. If this is the case, then we may have the first evidence that M68, which also exhibits a  $M/L_V$  peak near  $r_s$  and has a central concentration of 1.91 (van den Bergh 1995), is currently undergoing core collapse. Further observations are required, both photometric and kinematic, to confirm this.

Another important result from this study is the measured rotations of our clusters. Of the four clusters studied here, one exhibits an obvious rotation, namely M22, with an axis of rotation approximately North-South. M68 may be rotating as well and additional data are required to confirm this. M53 and M30 do not show any rotation to the level of  $0.5 \text{ km s}^{-1}$  and  $0.8 \text{ km s}^{-1}$  respectively.

While these results are strongly indicative of the current picture of globular clusters being dark matter poor, and their dynamics can be explained by standard Newtonian theory, we are currently undertaking robust dynamical modelling of GC systems to fully address the question of the influence of non-Newtonian physics in explaining our observations.

#### 5 ACKNOWLEDGMENTS

This project has been supported by the Anglo-Australian Observatory, the Australian Research Council and the Hungarian OTKA grant K76816.

#### REFERENCES

- Anderson, J. D., Laing, P. A., Lau, E. L., Liu, A. S., Nieto, M. M., & Turyshchev, S. G. 2002, *Phys. Rev. D*, 65, 082004
- Carney, B. W., Latham, D. W., Stefanik, R. P., Laird, J. B., & Morse, J. A. 2003, *AJ*, 125, 293
- Cole, A. A., Smecker-Hane, T. A., Tolstoy, E., Bosler, T. L., & Gallagher, J. S. 2004, *MNRAS*, 347, 367
- de Diego, J. A. 2008, *Revista Mexicana de Astronomia y Astrofisica Conference Series*, 34, 35
- Dejonghe, H. 1987, *MNRAS*, 224, 13
- Evstigneeva, E. A., Gregg, M. D., Drinkwater, M. J., & Hilker, M. 2007, *AJ*, 133, 1722
- Gregory, P. C. 2005, *Bayesian Logical Data Analysis for the Physical Sciences: A Comparative Approach with*

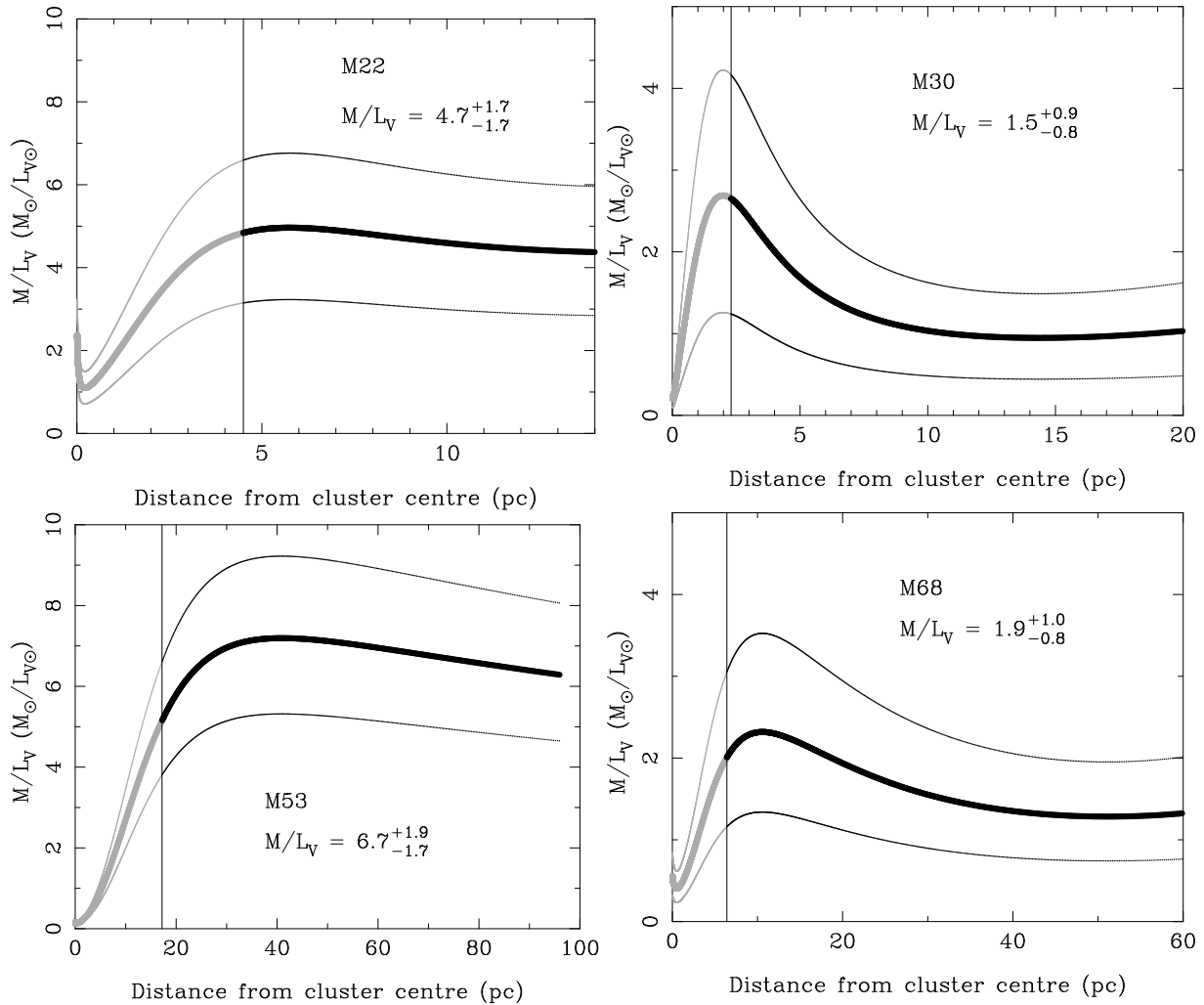


**Figure 4.** Mass-to-light profiles for each cluster (thick curve). The thin curves show the uncertainties on the  $M/L_V$ , calculated via the  $1\sigma$  difference of  $r_s$  from its calculated value. The vertical line indicates the value of  $r_s$ . The  $M/L_V$  value given is only calculated for radii greater than  $r_s$  because the mass estimates are highly uncertain in the cores of GCs, particularly if they are post-core-collapsed clusters.

‘Mathematica’ Support. Edited by P. C. Gregory. ISBN 0 521 84150 X (hardback); QA279.5.G74 2005 519.5’42 – dc22; 200445930. Published by Cambridge University Press, Cambridge, UK, 2005

Gunn, J. E., & Griffin, R. F. 1979, *AJ*, 84, 752

Harris, W. E. 1996, *VizieR Online Data Catalog*, 7195, 0

Hasegan, M., et al. 2005, *ApJ*, 627, 203

Ibata, R. A., Lewis, G. F., Irwin, M. J., & Quinn, T. 2002, *MNRAS*, 332, 915

Iorio, L. 2009, arXiv:0901.3011

Kiss, L. L., Székely, P., Bedding, T. R., Bakos, G. Á., & Lewis, G. F. 2007, *ApJL*, 659, L129

Mandushev, G., Staneva, A., & Spasova, N. 1991, *A&A*, 252, 94

Meziane, K., & Colin, J. 1996, *A&A*, 306, 747

Milgrom, M. 1983, *ApJ*, 270, 384

Moffat, J. W., & Toth, V. T. 2008, *ApJ*, 680, 1158

Moore, B. 1996, *ApJL*, 461, L13

Munari, U., Sordo, R., Castelli, F. and Zwitter, T. 2005, *A&A*, 442, 1127

Navarro, J. F., Frenk, C. S., & White, S. D. M. 1997, *ApJ*, 490, 493

Odenkirchen, M., et al. 2001, *ApJL*, 548, L165

Phinney, E. S. 1993, *Structure and Dynamics of Globular Clusters*, 50, 141

Plummer, H. C. 1911, *MNRAS*, 71, 460

Pryor, C., & Meylan, G. 1993, *Structure and Dynamics of Globular Clusters*, 50, 357

Scarpa, R., Marconi, G., Gilmozzi, R. and Carraro, G. 2007, *The Messenger*, 128, 41

Spitzer, L., Jr. 1985, *Dynamics of Star Clusters*, 113, 109

Steinmetz, M., et al. 2006, *AJ*, 132, 1645

Székely, P., Kiss, L. L., Sztatmáry, K., Csák, B., Bakos, G. Á., & Bedding, T. R. 2007, *Astronomische Nachrichten*, 328, 879

Trager, S. C., King, I. R., & Djorgovski, S. 1995, *AJ*, 109, 218

Webbink, R. F. 1981, *ApJS*, 45, 259

van den Bergh, S. 1995, *AJ*, 110, 1171

Zwitter, T. et al. 2008, *AJ*, 136, 421